Amino Acid-Assisted Solvothermal Synthesis of LiFePO$_4$ Cathode Materials

Amin Sarmadi, Seyyed Morteza Masoudpanah, Somaye Alamolhoda*

School of Metallurgy & Materials Engineering, Iran University of Science and Technology (IUST), Narmak, Tehran, Iran.

*Corresponding author email: alamolhoda@iust.ac.ir

ABSTRACT

In the energy storage field, lithium-ion batteries were known to be the most important approach for mitigating the environmental impacts of fossil fuels. Cathode materials are the crucial part of a lithium-ion battery, and LiFePO$_4$ (LFP) cathode material was selected for its high voltage (3.45 V vs. Li+/Li), high theoretical capacity (170 mAh.g^{-1}), significant cyclic stability, and environmental friendliness. On the contrary, the main downside of LFP materials is their one-dimensional lithium-ion diffusion channel at the crystallographic direction of [010]. These channels can be blocked by antisite defects, plunging the specific capacity of LFP materials. Thus, in order to reduce such impacts, having sheet-like morphologies with a significant crystallographic plane of (010) is essential. A great deal of research has been performed using a solvothermal method for the synthesis of LFP materials, and factors - as precursors, pH of the solution, temperature, time, and additives - were known to have significant roles in the structural as well as electrochemical properties of LFP materials. In this study, different amounts of the amino acids, namely glycine and glutamic acid, were introduced in the solvothermal synthesis of LFP materials, and their respective roles in morphology and electrochemical characteristics were investigated. The self-assembled morphology of LFP particles using glycine was discussed by the formation of peptide bonds. Additionally, having another carboxylic acid group in the molecular structure of glutamic acid sustained a low pH in the solvothermal solution; therefore, the formation of self-assembled morphology could not occur during the synthesis process. Additionally, the specific capacity of the LFP/C materials after the heat treatment was discussed by Rietveld refinement investigations for determining the antisite defects.

Keywords: *Solvothermal synthesis, LiFePO$_4$, Amino acid, Morphology.*

1. Introduction

An important consequence of using fossil fuels is the emission of CO$_2$ gas and global warming. One way to mitigate this effect is to utilize rechargeable batteries, which can restore electrical energy in the form of chemical reactions [1,2]. In the field of lithium-ion batteries, great efforts have been made to find alternatives to the cobalt-based cathode materials for large-scale applications (e.g. electric vehicles) [3-5]. Olivine-structured materials such as LFP are promising cathode materials owing to their advantages, namely medium operating voltage (about 3.5 V vs. Li / Li $^+$), large theoretical capacity (170 mAh.g^{-1}), and low cost. Moreover, compared to the cobalt-based cathode materials, LFP is non-toxic and much safer for use in lithium-ion batteries [6,7]. One of the biggest obstacles to the widespread use of LFP is its inherent lack of conductivity. Different methods have been used to overcome this barrier, from which the use of conductive coatings and grain size reduction had been recommended. Reducing the size of

particles to nanoscale or less than microns along the 1-dimensional lithium-ion diffusion channels in LFP improves its electrochemical performance. In addition, reducing the crystallite size reduces the mechanical strain of the lattice [8,9].

Solid state reactions were used as a suitable method for the production of LFP, but the problems with this synthesis method are the considerable energy consumption and uncontrolled grain growth. With the solution method, the controlling morphology of the products can be easily adjusted, and the energy consumption is low since part of the synthesis process can be performed in the solution medium. Further, phase purity and crystal defect concentration are the other characteristics that can be adjusted by changing the parameters of solvothermal synthesis, namely by an alternation of pH, temperature, time, and the use of surfactants and additives 10-16].

Reducing the particle size of LFP in the specific crystallographic direction of [010], which is a preferred direction for the diffusion of Li in the crystal structure, can improve the diffusion performance. Besides the lack of conductivity, the presence of anti-site defects lowers the specific capacity of LFP materials, consequently making ineffective segments of lithium ions in the olivine structure. The use of organic solvents not only improve the nucleation of the particles during the solvothermal process but also reduces the antisite defects. Due to the poor conductivity of this material, carbon coating is commonly used; the use of carbon coating can be done during the calcination process. If different organic solvents

and additives graft onto the surface of the particles, they can be converted to conductive carbon during the calcination process [17-19].

In this research, two types of additives have been used to achieve the appropriate grain size and morphology. The additives used are the amino acids glycine and glutamic acid and their effects on the electrochemical performance of LFP material were investigated. These types of amino acids have been studied due to the presence of carboxylic acid and amine functional groups in their molecular structure. The effects of adding these amino acids separately and in different ratios on the solvothermal synthesis of LFP have been investigated. This study was focused on the functional groups of amines and carboxylic acids and the effects in which these additives can change the pH of the solution owing to the zwitterion effect and the resulting interactions in the form of peptide bonds between amino acids to produce different morphologies in solvothermal reactions have been considered. The amino acid glycine, due to the lack of an R chain, contains only one carboxylic acid and one amine, and its isoelectric point is equal to 6. Glutamic acid consists of two groups of carboxylic acids and one group of amines. The presence of two carboxylic acid functional groups in glutamic acid causes the isoelectric point of this amino acid to be low and equal to 3 (Fig.1). The tendency to absorb or lose H^+ ions in the functional groups of amino acids by changing the pH is known as zwitterionic property. Zwitterionic properties in amino acids can be used as a feasible factor due to the tendency to bring the pH closer to the isoelectric point and keep the
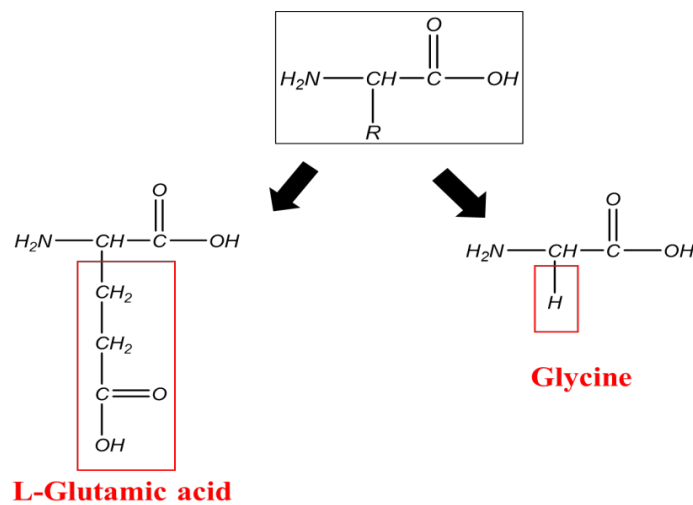

Fig. 1- The two types of amino acids used in this study have two different types of R chains.

pH constant in solution during the solvothermal process. Because the pH of the solution changes over time during the solvothermal process [20], zwitterionic properties can assist researchers to better investigate the effects and benefits of a constant pH through a solvothermal process.

Initially, for proving the formation of the LFP phase after the solvothermal process, XRD phase analysis of the synthesized samples was performed. The effects of particle shape and antisite defects on the electrochemical properties of LFP particles have also been investigated. The electrochemical experiments included in this study are galvanostatic study and capacity stability in multiple cycles. Electrochemical charge and discharge were performed to evaluate the performance of the materials. In order to elicit the reasons for increasing the charge and discharge capacity, Rietveld refinement method has been used.

2. Experimental details
2.1. Synthesis

All precursors of LiOH, FeSO4.7H2O, H3PO4 (85 wt.%), glycine ($C_2H_5NO_2$), and l-glutamic acid ($C_5H_9NO_4$) were purchased from Merck Co.

In order to find the optimal amount of additives, different ratios of glycine and l-glutamic acid have been used. The amounts of glycine and l-glutamic acid added for solvothermal synthesis is shown in Table 1. From Table 1, it can be seen that as the amount of glutamic acid increases, the pH remains constant at 2. As the amount of glycine in the solution increases, it is observed that the pH value approaches the isoelectric value of glycine.

Firstly, 25 mmol FeSO4.7H2O dissolved in 30 ml ethylene glycol at 80 °C. Then, different ratios of glycine and l-glutamic acid were separately added into the FeSO4 solution according to Table 1. In the meantime, 25 mmol H3PO4 was dropwisely added to 75 mmol LiOH aqueous solution (30 mL) under the magnetic stirring condition at 80 °C, from which white precipitation eventually resulted. Next, the two above solutions were mixed to form an opaque blue gel-like precursor which

was poured into a 100 ml Teflon lined stainless steel autoclave and heated at 180 °C for 6 h similar to our previous work [21]. The obtained precipitates were washed three times with distilled water and ethanol then mixed with 20 wt. % sucrose as the carbon source and finally calcined at 700 °C for 6 h under Ar flow atmosphere. The various samples were coded according to the amount of l-glutamic acid and glycine used for the synthesis, as shown in Table 1.

2.2. Material characterization methods

The crystal structure of different samples was characterized by powder X-ray diffraction (XRD) using an X-ray diffractometer D8 ADVANCE instrument (Bruker, Germany). The CuKα (λ = 1.54060 Å) was irradiated for scanning the powder in the diffraction angles of 2q=10- 80° at a scan speed of 0.02°/1 s. Rietveld refinement was carried out by GSAS-II software to calculate the crystal parameters [22]. Scanning electron microscopy (SEM) images were taken by a Vega II microscope (TESCAN, Czech Republic).

2.3. Electrochemical characterization

The LFP active material, polyvinylidene fluoride binder, and carbon black were mixed in a weight ratio of 70:15:15 in N-methyl pyrrolidone (NMP) solvent. The slurry was tape casted on Al foil as the positive current collector. The mass density of LFP was 2 mg cm^{-2} following the evaporation of NMP solvent. The coin cell (2016 type) was assembled inside an Ar filled glovebox by using Li foil as anode and 1 M LiPF6 in a 1:1 ethylene-carbonate (EC) /diethyl-carbonate (DEC) mixture as solvent. Galvanostatic charge/discharge tests were conducted in the potential range of 2.0- 4.2 V vs. Li$^+$/Li at various C rates on a BTS-5V 10mA battery tester (NEWARE, China).

3. Results and discussion
3.1. Crystal structure

XRD patterns of the samples synthesized by glycine and l-glutamic acid are shown in Fig. 2. G2 and G3 samples contains $Fe_{4.7}P_4O_{20}$ impurity.

Table 1- The amount of glycine and glutamic acid used in the experiments and the amount of pH measured after the solvothermal process of the remaining solution

Amino acid	Glycine			L-glutamic acid			No amino acid
mmol	12.5	25	50	12.5	25	50	0
Code	G1	G2	G3	E1	E2	E3	NA
pH	2	3	4	2	2	2	2

The impurity obtained is similar to the impurity observed in the NA sample. For the l-glutamic acid samples, it also can be seen that the samples have $Fe_{4.7}P_4O_{20}$ impurity. Fig. 2 shows that the impurity peaks become sharper with the increasing amount of glutamic acid.

Rietveld method was used to investigate the presence of antisite defects in LFP particles of NA, E2, and G2 samples (Fig. 3). No impurities were observed in the obtained XRD patterns after calcination of all samples and the unit cell volume of NA is equal to 292.811 $Å^3$ (Fig. 3). G2 sample has a unit cell volume of 289.251 $Å^3$, exhibiting a great decrease compared to NA sample. Due to the decrease in unit cell volume from 291.4 $Å^3$ [23], representing a defect-free sample, the possibility of Fe^{3+} ions can be predicted in a very small amount in the structure[24]. The unit cell parameters calculated using Rietveld method for E2 sample

are shown in Fig. 3. The volume of a single cell in the use of glutamic acid is equal to 292.107 $Å^3$, indicating the presence of $Li_{Fe}^{-}+ Fe_{Li}^{.}$ antisite defects in the structure [23]. The sample without amino acids, shown in Fig. 3, has a unit cell volume
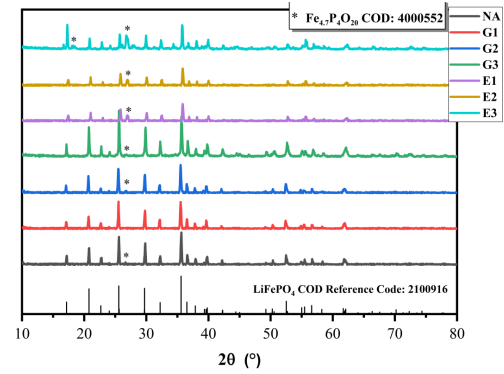

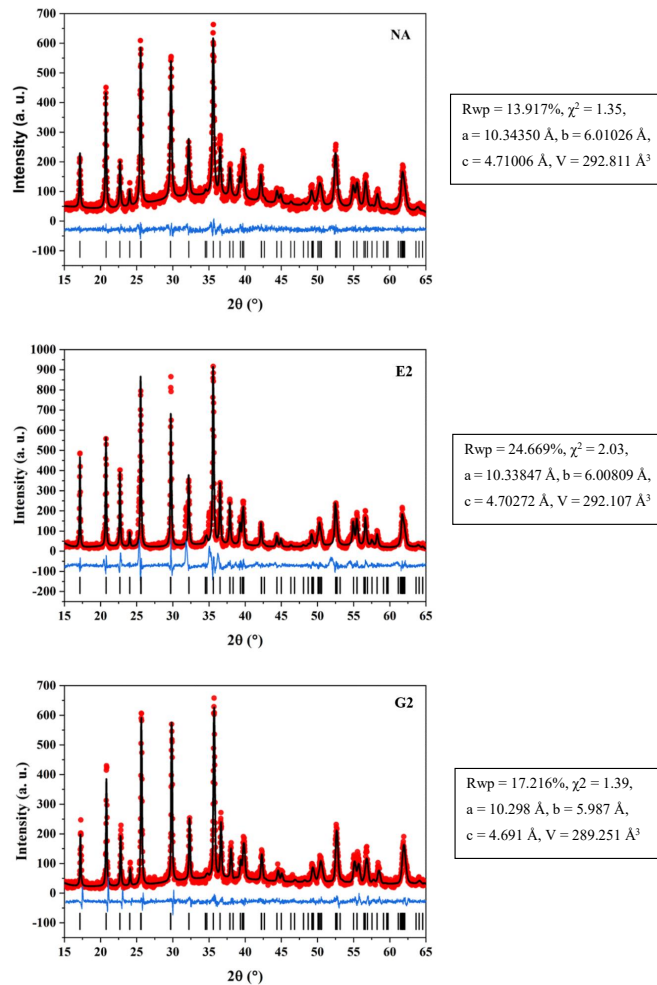Fig. 2- XRD patterns for NA, G1, 2, 3, and E1, 2, 3 samples.

Fig. 3- The investigation of antisite defects from XRD patterns after calcination for NA, E2, G2 samples.

of 292.811 $Å^3$, indicating a small increase in unit cell volume compare to the E2 sample.

3.2. Morphology

The SEM images of NA, G2, and E2 samples are shown in Fig. 4. The SEM images reveal that the particles obtained from the addition of the amino acid glycine are large secondary particles obtained from smaller primary plate particles. On the other hand, the morphology obtained from the sample without adding amino acids was observed as flake-like particles. It can be inferred that using glycine leads to the agglomeration of flakes particles next to each other in an orderly manner. The reason for this phenomenon can be attributed to the addition of the amino acid glycine making it possible to form peptide bonds during synthesis. The particle thickness seen in Fig. 4f is about 170 nm. Fig. 4g, h, i show that compared to the results obtained from the samples of glycine, which

showed a significant change in the morphology of the particles, the addition of l-glutamic acid to the solvothermal solution had no effect. The reason for this phenomenon may be related to the molecular structure of l-glutamic acid compared to the other sample. The thickness of the sheet observed in the SEM image of Fig. 4i is about 140 nm. The presence of two groups of carboxylic acids introduced an acidic condition into the solution of the solvothermal process. The acidic nature of the solution also intensifies Ostwald ripening process in the particles [25]. This phenomenon causes the resulting particles to be seen as large sheet-shaped particles. It is also possible that due to the acidity of the solution, the formation of peptide bonds was precluded during the solvothermal synthesis. When l-glutamic acid was added to the solution, it does not lose the hydrogen in the carboxylic acid group owing to the zwitterionic property of the amino acids. Therefore, one of the factors for the
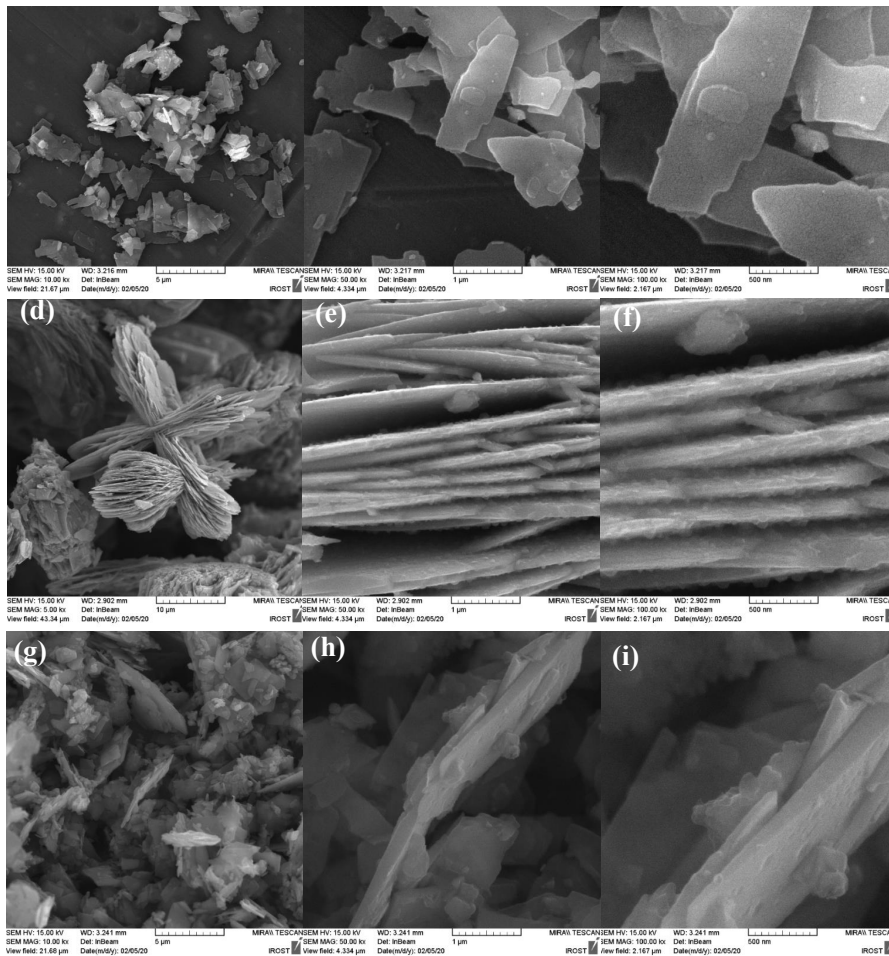

Fig. 4- The SEM images for (a,b,c) NA, (d,e,f) G2, and (g,h,i) E2 samples at different magnifications.

formations of peptide bonds was removed and no change was observed in the obtained morphology (Fig. 5).

3.3. Specific capacity

The electrochemical capacities obtained from the samples were shown in Fig. 6. The specific capacity at the rate of 0.2C for the samples G1, 2, and 3 is equal to 16, 26, and 4 mAh.g^{-1}, respectively (Fig. 6 (c)). According to the obtained results, although showing a poorer electrochemical performance than NA for 0.5, 1, 2, 5C rates, the capacity of G2 is equivalent to NA at 10C and shows a slight increase at 0.2C than NA afterward. Fig. 6 (b) shows the different charge / discharge curves at different C rates for G2 sample. In all rates except 5C and 10C showing a pseudo-capacitive behavior, a two-phase constant voltage zone is observed [9].

The electrochemical results obtained from the addition of glutamic acid in the solvothermal synthesis are shown in Fig. 6 (d). The results of the specific capacity show that E2 sample has the highest specific capacity among different ratios of glutamic acid added. The capacities at C rates of 0.2, 0.5, 1, 2, 5, 10C are equal to 16, 11, 9.5, 7, 6 and 5 mAh.g^{-1} respectively. The E2 sample at higher rates shows a more severe capacity reduction than the other samples, and at a rate of 10C, the capacity is approximately equal to that of the other samples. It is observed that unlike the addition of glycine, which shows an increased specific capacity at 0.2C rate, the addition of l-glutamic acid reduces the specific capacity of LFP particles synthesized without amino acids. In Fig. 6 (e), similar to the results obtained from glycine samples, there is no two-phase zone with increasing charge / discharge rate for 5 and 10C, and it has pseudo-capacitive behavior [9]. Comparing the curves obtained from the samples used with glycine and glutamic acid, it is observed that the addition of glutamic acid has an adverse effect on the specific capacity of LFP.

4. Conclusion

According to the SEM images, the final particles obtained from the G2 sample are in the form of LFP particles synthesized without amino acids stacked together regularly, which may be due to the peptide bonds formation during solvothermal synthesis. In order to investigate the function of different amino acids on the solvothermal synthesis of LFP, electrochemical experiments were used. The glycine sample has a large grain size feature and a decrease of unit cell volume due to the presence of Fe^{3+} ions in its structure. Also, it was observed that the addition of glutamic acid due to the presence of an additional carboxylic acid group tends to keep the pH of the solution low and near to its isoelectric point. Therefore, peptide bonding, which was assumed to be a factor in achieving such hierarchical morphology obtained in glycine, was not formed. Also, based on the unit cell volume of E2 sample, the addition of glutamic acid had no considerable effect on reducing antisite defects. Except for G2 sample which shows a slight increase at additional cycles, the specific capacity obtained from other samples is close to that of no amino acid sample and even lower.
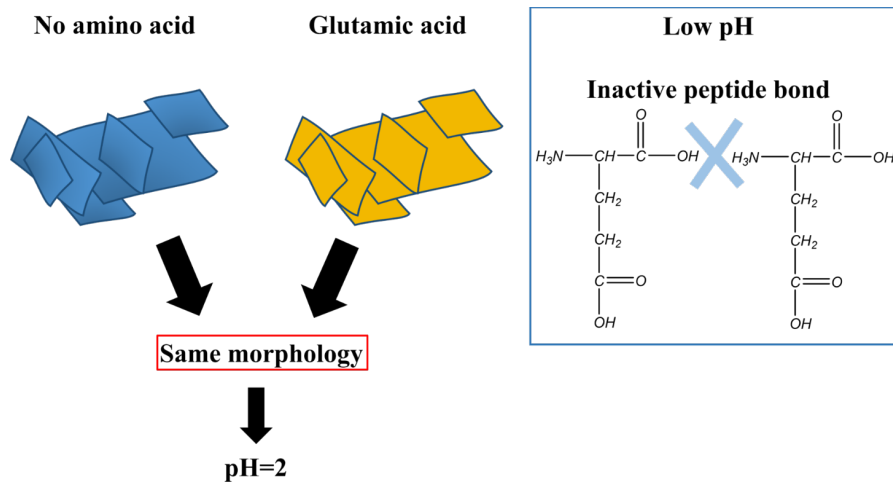

Fig. 5- Schematic for explaining the same morphology of E2 and NA samples because of the low pH and inactive peptide bond.
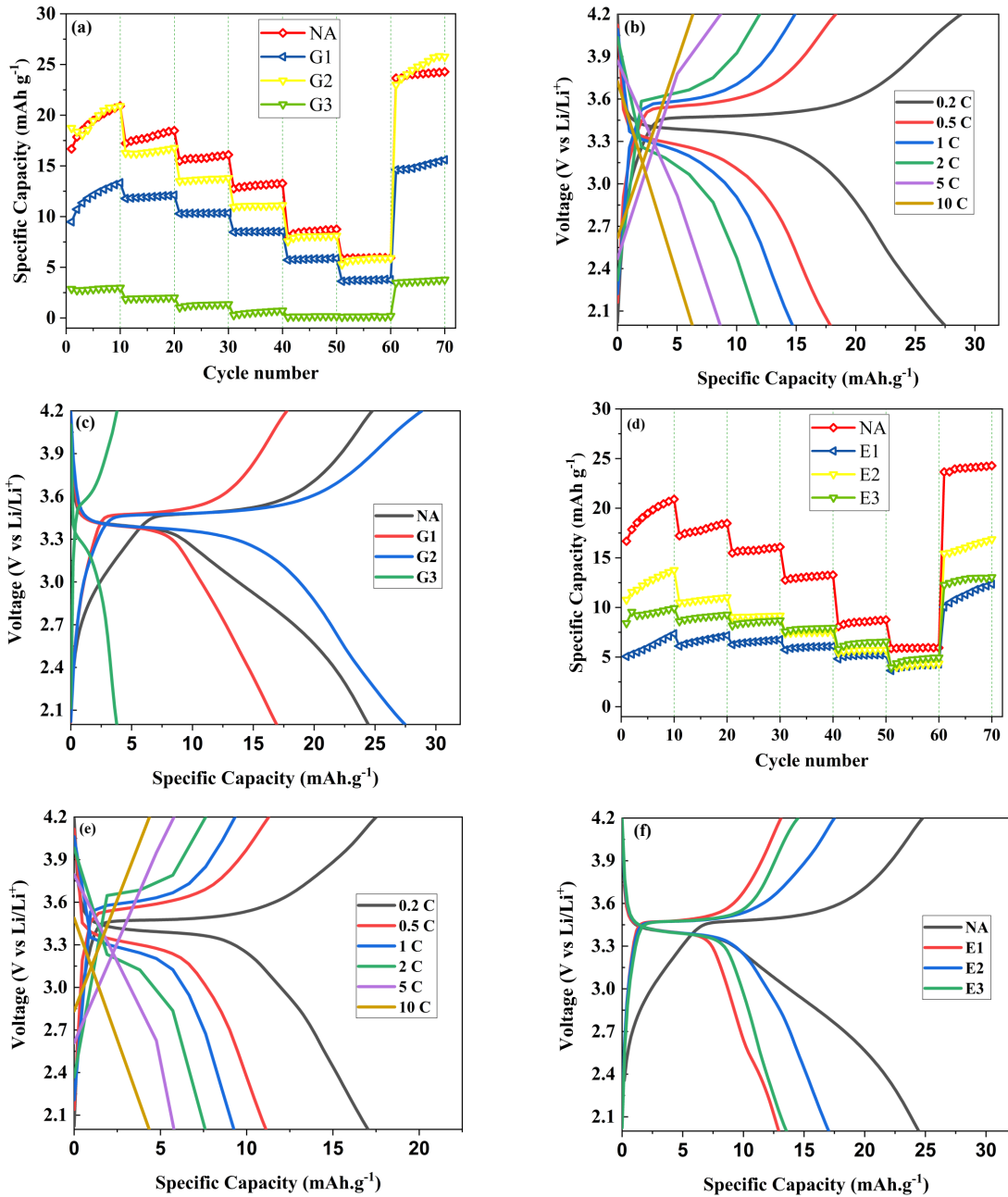
Fig. 6- Results of specific capacity obtained from (a) glycine and (d) l-glutamic acid at different charge and discharge rates, charge / discharge curves at different rates for (b) G2 and (e) E2 samples which had the highest capacity, and the comparison of charge and discharge curves of the (c) glycine and (f) l-glutamic acid samples with no amino acid sample at 0.2C rate.

References

1. Liu S, Kang L, Hu J, Jung E, Zhang J, Jun SC, et al. Unlocking the Potential of Oxygen-Deficient Copper-Doped Co3O4 Nanocrystals Confined in Carbon as an Advanced Electrode for Flexible Solid-State Supercapacitors. ACS Energy Letters. 2021;6(9):3011-9.

2. Liu S, Kang L, Jun SC. Challenges and Strategies toward Cathode Materials for Rechargeable Potassium-Ion Batteries. Advanced Materials. 2021;33(47):2004689.

3. Andre D, Kim S-J, Lamp P, Lux SF, Maglia F, Paschos O, et al. Future generations of cathode materials: an automotive industry perspective. Journal of Materials Chemistry A. 2015;3(13):6709-32.

4. Liu S, Kang L, Zhang J, Jun SC, Yamauchi Y. Carbonaceous Anode Materials for Non-aqueous Sodium- and Potassium-Ion Hybrid Capacitors. ACS Energy Letters. 2021;6(11):4127-54.

5. Liu S, Kang L, Zhang J, Jung E, Lee S, Jun SC. Structural engineering and surface modification of MOF-derived cobalt-

based hybrid nanosheets for flexible solid-state supercapacitors. Energy Storage Materials. 2020;32:167-77.

6. Sławiński WA, Playford HY, Hull S, Norberg ST, Eriksson SG, Gustafsson T, et al. Neutron Pair Distribution Function Study of FePO4 and LiFePO4. Chemistry of Materials. 2019;31(14):5024-34.

7. Manthiram A. An Outlook on Lithium Ion Battery Technology. ACS Cent Sci. 2017;3(10):1063-9.

8. Malik R, Burch D, Bazant M, Ceder G. Particle Size Dependence of the Ionic Diffusivity. Nano Letters. 2010;10(10):4123-7.

9. Eftekhari A. LiFePO4/C nanocomposites for lithium-ion batteries. Journal of Power Sources. 2017;343:395-411.

10. Sharikov FY, Drozhzhin OA, Sumanov VD, Baranov AN, Abakumov AM, Antipov EV. Exploring the Peculiarities of LiFePO4 Hydrothermal Synthesis Using In Situ Calvet Calorimetry. Crystal Growth & Design. 2018;18(2):879-82.

11. Jiang Y, Tian R, Liu H, Chen J, Tan X, Zhang L, et al. Synthesis and characterization of oriented linked LiFePO4 nanoparticles with fast electron and ion transport for high-power lithium-ion batteries. Nano Research. 2015;8(12):3803-14.

12. Benedek P, Wenzler N, Yarema M, Wood VC. Low temperature hydrothermal synthesis of battery grade lithium iron phosphate. RSC Advances. 2017;7(29):17763-7.

13. Huang X, Zhang K, Liang F, Dai Y, Yao Y. Optimized solvothermal synthesis of LiFePO4 cathode material for enhanced high-rate and low temperature electrochemical performances. Electrochimica Acta. 2017;258:1149-59.

14. Cho M-Y, Kim H, Kim H, Lim YS, Kim K-B, Lee J-W, et al. Size-selective synthesis of mesoporous LiFePO4 microspheres based on nucleation and growth rate control of primary particles. J Mater Chem A. 2014;2(16):5922-7.

15. Chen M-m, Ma Q-q, Wang C-y, Sun X, Wang L-q, Zhang C. Amphiphilic carbonaceous material-intervened solvothermal synthesis of LiFePO4. Journal of Power Sources. 2014;263:268-75.

16. Fischer MG, Hua X, Wilts BD, Castillo-Martínez E, Steiner U. Polymer-Templated LiFePO4C Nanonetworks as High-Performance Cathode Materials for Lithium-Ion Batteries. ACS Applied Materials & Interfaces. 2018;10(2):1646-53.

17. Zhao Y, Peng L, Liu B, Yu G. Single-Crystalline LiFePO4 Nanosheets for High-Rate Li-Ion Batteries. Nano Letters. 2014;14(5):2849-53.

18. Li W, Wei Z, Huang L, Zhu D, Chen Y. Plate-like LiFePO 4 /C composite with preferential (010) lattice plane synthesized by cetyltrimethylammonium bromide-assisted hydrothermal carbonization. Journal of Alloys and Compounds. 2015;651:34-41.

19. Martinez PS, Lima E, Ruiz F, Curiale J, Moreno MS. Morphology and Electrochemical Response of LiFePO4 Nanoparticles Tuned by Adjusting the Thermal Decomposition Synthesis. The Journal of Physical Chemistry C. 2018;122(33):18795-801.

20. Zhu J, Fiore J, Li D, Kinsinger NM, Wang Q, DiMasi E, et al. Solvothermal Synthesis, Development, and Performance of LiFePO4 Nanostructures. Crystal Growth & Design. 2013;13(11):4659-66.

21. Sarmadi A, Masoudpanah SM, Alamolhoda S. L-Lysine-assisted solvothermal synthesis of hollow-like structure LiFePO4/C powders as cathode materials for Li-ion batteries. Journal of Materials Research and Technology. 2021;15:5405-13.

22. Toby BH, Von Dreele RB. GSAS-II: the genesis of a modern open-source all purpose crystallography software package. Journal of Applied Crystallography. 2013;46(2):544-9.

23. Whittingham MS. Ultimate Limits to Intercalation Reactions for Lithium Batteries. Chemical Reviews. 2014;114(23):11414-43.

24. Liu Y, Zhang J, Li Y, Hu Y, Li W, Zhu M, et al. Solvothermal Synthesis of a Hollow Micro-Sphere LiFePO₄/C Composite with a Porous Interior Structure as a Cathode Material for Lithium Ion Batteries. Nanomaterials (Basel). 2017;7(11):368.

25. Lu Z, Chen H, Robert R, Zhu BYX, Deng J, Wu L, et al. Citric Acid- and Ammonium-Mediated Morphological Transformations of Olivine LiFePO4 Particles. Chemistry of Materials. 2011;23(11):2848-59.